Military Technical College
Kobry El-Kobbah,
Cairo, Egypt.

17th International Conference
on Applied Mechanics and
Mechanical Engineering.

THE EFFECT OF TANTALA AND NIOBIA ADDITION ON THE PHYSICAL AND MECHANICAL PROPERTIES OF α ALUMINA CERAMICS

S. M. Naga*, M. Awaad* and A. M. Hassan**

ABSTRACT

The effects of Ta_2O_5 and Nb_2O_5 addition on the densification behavior, microstructure and mechanical properties of Al_2O_3 ceramics were investigated. The Ta_2O_5 and Nb_2O_5 additions to the alumina matrix were varied from 0.25wt% to 0.75 wt%. The powders of each composition were uniaxially pressed at 220 MPa into discs and rectangular bars, then pressureless-sintered at 1650 °C for 1 h. The phase constitution and microstructure of the sintered ceramic bodies were characterized with a X-ray diffractometer and a SEM. The mechanical properties of the ceramic bodies were evaluated on the basis of their Vickers hardness (HV1), bending strength and fracture toughness. It was found that Ta_2O_5 addition enhanced the mechanical properties of alumina bodies in comparison to Nb_2O_5 addition. The maximum bending strength, fracture toughness and Vickers hardness of the bodies with 0.75wt% Ta_2O_5 were 14.2, 6.1 and 3% higher than that of 0.75 wt% Nb_2O_5 doped Al_2O_3 samples.

KEY WORDS

Doping, Alumina, Tantala, Niobia, Microstructure.

* Professor, Dept. of Ceramics, National Research Center, Cairo, Egypt.
** Lecturer, Dept, of Materials Engineering, Faculty of Engineering, Zagazig University, Zagazig, Egypt.

INTRODUCTION

Alumina oxide attracted the attention of researchers due to its unique mechanical, electrical and optical properties. It is well known that properties of alumina influenced by trace impurities and additives [1,2]. The influence of rare earth oxides additions on the alumina properties was widely studied [3-9]. Odaka et al [9] reported that doping of Al_2O_3 with nanopowder rare earth oxides enhanced the densification at low temperature. They claimed that the synergistic effect between the nano-sized alumina particles and suppression effect of the homogenously segregated rare earth dopant on the alumina grain growth are the reasons of the excellent low temperature densification of rare earth/alumina doped bodies. On the other hand, Wang et al [8] showed that Nd_2O_3 doping inhibited Al_2O_3 densification. Fang et al [10] believed that the densification inhabitation is due to the suppression of grain-boundary diffusion resulted from the segregation of the rare earth ions misfitted to the Al_2O_3 grain boundaries.

Many authors studied the effect of rare earth dopants on the alumina body's mechanical properties [6,11,12]. Rani et al [6] and Xu et al [12] reported that rare earth ions (Yb^{3+}, Er^{3+} and La^{3+}) improve the mechanical properties of alumina. They showed that the formation of anisotropic elongated grains results in crack bridging and crack deflection that in turn improve the fracture toughness of the Al_2O_3 doped bodies. The present article mainly analyzes the effect of both Nb_2O_5 and Ta_2O_5 doping on the microstructure, mechanical and physical properties of alumina ceramics. Nb_2O_5 and Ta_2O_5 were added separately to alumina in a range of 0.25 up to 0.75 wt%.

MATERIALS AND METHODS

Materials and Processing

Compositions of Nb_2O_5- and Ta_2O_5- doped alumina were prepared on the basis of powder mixing according to Table. 1. The Al_2O_3 used had 99.98% purity (provided by Almatis Gmbh Ludwigshafen/RH, Germany), and both niobium and tantalum oxides had 99.9% purity (provided by SIGMA-ALDRICH chemistry, USA). The particle size of the as-received Al_2O_3, Nb_2O_5 and Ta_2O_5 is ranged between 135-150 nm and 100-120 nm respectively. All powders were mechanically mixed using a ball mill for 5 h using 5 mm zirconia balls and a polypropylene container with constant speed of 300 rpm. The obtained powders were formed by uniaxial pressing at 220 MPa into discs of 13 mm in diameter and 4 mm in height (for physical and microstructural characterization) and rectangular bars of dimensions of 6 x 6 x 60 mm^3 (for mechanical evaluation). The bodies formed were pressureless - sintered in an electric oven at 1650 ºC for one-hour soaking time. Heating and cooling rates were 5 ºC/min.

Characterization

Relative density was used to evaluate the densification behavior, while the developed phases were identified by X-ray diffraction analysis (XRD). The microstructure of the fractured surfaces of the sintered specimens was examined with scanning electron microscope (SEM-Jeol JSM-T20). The Vickers hardness of the sintered samples was measured with hardness tester (Omnimet automatic MHK system Model Micro Met 5114, Buehler USA). 30 indents were made for each sample and average hardness was calculated according to the following equation [13]:

$$H = 1.8544\ (P/d^2) \qquad (1)$$

where p is the load and d is the length of the impression diagonal.

Bending strength was measured in a three-point bending test on a universal testing machine, the fracture toughness was determined with the single- edge v- notched beam (SEVNB) technique [14]. The fracture toughness was determined by applying the following equation [15]:

$$K_{1c} = [P_{max} / t\ (h^{1/2})] \times [L_0 - L_i/h] \times [3R_M\ (d/h)^{1/2} /\ 2(1 - d/h)^{3/2}] \qquad (2)$$

where, P_{max} is the maximum load (N), L_0 and L_i are the outer and inner roller spans (mm); respectively, t and h are thickness and height of the specimen (mm), d is the depth of the sharpened notch (mm).

$$R_M = [1.9887 - 1.326\ (d/h) - [3.49 - 0.68\ (d/h) + 1.35\ (d/h)^2]\ (d/h)\ (1-(d/h)] / (1 + (d/h))^2 \qquad (3).$$

RESULTS AND DISCUSSION

Physical Properties and Phase Composition

The effect of pentavalent oxides (Nb_2O_5 and Ta_2O_5) doping on the relative density of the studied bodies is shown in Fig. 1. The figure shows that the increase in the dopants content increases the relative density of the obtained bodies fired at 1650ºC from 92.97 (X0) up to 98.66% (X3) and 98.75% (X6). The fine particle size of the dopants yields better powder flow ability and packing density, leading to higher green density values [16]. It was mentioned that the driving force for diffusion is increased by the increase in the specific surface area. It leads to the increase in the number of contact points between dopants and the alumina matrix, which in turn reduces the diffusion paths. Fine, dispersed pentavalent dopants occupying the voids between alumina particles have the effect of pinning the alumina and prevent grain growth [16]. Ta_2O_5 doped ceramics possess better relative density values compared to the Nb_2O_5 doped samples. This behavior is attributed to the solid solution formed at the grain-boundary triple junctions of alumina matrix of the Nb_2O_5 doped alumina samples, Fig.2. Some authors [17, 18] claimed that the formation of amorphous glassy phase near the crystallized alumina grains hinders the diffusion of dopants into the alumina matrix. It forms an intergranular liquid phase that enhances the abnormal grain growth and leads to the trapping of pores within and between the abnormally grown alumina particles. Figure 3.a &b illustrates the effect of the grain size on the densification behavior of the alumina doped bodies.

The figure shows that the average grain size of Ta^{5+} doped samples is smaller than that of Nb^{5+} samples (6,11 µm respectively). It indicates that Ta^{5+} ions suppression the alumina grain growth and enhances the samples densification [6].

Figs. 4a & b. show the XRD patterns of the fired alumina/ Nb_2O_5 and Ta_2O_5 bodies. The figure shows that the alumina phase is the dominant phase present in the Nb_2O_5 doped bodies. The shift in the alumina peaks indicates the formation of a solid solution between alumina and Nb_2O_5. The higher d values and lower 2θ shift are clearly shown in the XRD patterns of X2 and X3 samples, with 0.5 and 0.75% Nb_2O_5, Fig. 4a. In several studies of the binary Al_2O_3 system [19], Nb_2O_5 - Al_2O_3 compounds have been reported to occur at molar ratios of 1:1, 1:9, 1:11, 1:25 and 1:49. The most suggested binary compounds are at 1:1, 1:11, and 1:49 molar ratios. The structure of Al NbO_4 is built from distorted [NbO_6] and [AlO_6] octahedral sharing edges and corners, and linked together to give an infinite three-dimensional network [20]. XRD patterns of the fired alumina/ Ta_2O_5 bodies; Fig. 3b; illustrates that all detectable diffraction peaks are corresponding to those of α- Al_2O_3. The tantalum oxide phase is also present in a very minute proportion compared to the bulk Al_2O_3.

Microstructure

Figures 5 a, b, c and d show the microstructure features of the pure alumina and alumina bodies doped with 0.25, 0.5 and 0.75wt% Nb_2O_5 and sintered at 1650 ℃. Abnormal grain growth is noticed in the pure alumina samples. While, alumina grains of the sample doped with 0.25wt% Nb_2O_5 mostly exhibit an equiaxed shape. With the increase of Nb_2O_5 content, the grains tend to show abnormal grain growth. The figure shows that in contrast to the approximately uniform microstructure of the X1 sample, the grain structure of X2 and X3 samples is bimodal, comprising coarse grains and fine grains. The microstructure of the samples with different Nb_2O_5 concentrations shows that some of the triple junctions are occupied by bright particles, which are Nb_2O_5, while some other Nb_2O_5 particles are present in the intragranular position within the alumina grains. The microstructure of Ta_2O_5 doped alumina samples; Fig. 6 (a, b and c); shows that it consists of two types of grains. The small grains having a nearly square shape are Ta_2O_5 grains, and the large grains having irregular geometry including elongated shape are Al_2O_3 grains. Fig. 6a shows that alumina grains are completely enclosed by tiny Ta_2O_5 grains. The grain size of the Ta_2O_5 ranges between 647 and 29.14 nm. Figures 6b and c show that with the increase in the Ta_2O_5 content some of the Ta_2O_5 dopants were consumed in the formation of Ta_2O_5 islands.

Mechanical Behavior

Bending strength

The bending strength of Al_2O_3 doped with Nb_2O_5 or Ta_2O_5 is higher than that of undoped specimens (Fig. 8). We believe that the increase in the bending strength of the doped samples is attributed to the addition of rare earth oxides. As shown in Fig. 1 the addition of Nb_2O_5 increases the fired samples' relative density, which in turn enhances the bending strength of the bodies [21]. At the same time, the presence of the dopant particles reduces the crack length by forming sub-boundaries in the matrix grains could be afforded to the difference in the expansion coefficient of the phases conforming the body, Ta_2O_5 (6.72×10^{-6}/℃ in 0–1000℃), Nb_2O_5 (5.9× 10-6/℃ in 0–

1000 °C) and Al_2O_3 (8.8×10-6/°C in 0–1000°C) [22]. Such difference in the thermal expansion enhances the bending strength by inducing residual tension in Nb_2O_5 or Ta_2O_5 phases and residual compression in the Al_2O_3 matrix after cooling [21]. The increase in the bending strength of Ta_2O_5 doped samples in comparison to those doped with Nb_2O_5 is due to the improvement of the densification parameters of the Ta_2O_5 doped samples.

Vickers hardness

Figure.9 indicates that the increase in the dopants content increases the hardness of the samples. The doped bodies showed remarkable improvement in hardness at all Nb_2O_5 and Ta_2O_5 concentrations over that of the pure alumina samples. The maximum hardness of Al_2O_3 /0.75 wt% Ta_2O_5 (1522) was 33.4% higher than that of pure alumina (1141) and 3% higher than that of Al_2O_3 /0.75 wt% Nb_2O_5 samples (1478). Also, with lower percentages of doping Ta_2O_5 doped samples showed higher hardness' percentages than that of Nb_2O_5. This behavior could be attributed to the difference in the relative density of the two composites. It was reported that porosity reduces the hardness of ceramic materials by producing stress concentration points, which are a crack initiation points [23,24].

Fracture toughness

The fracture toughness of the samples increases with the increase in Nb^{5+} and Ta^{5+} ions contents. The increase in the fracture toughness values is a reflection of both the densification and microstructure. Formation of anisotropic elongated grains (Fig. 2), can result in crack bridging and crack deflection. On the other hand, dislocation lines, dislocation rings, dislocation twisting and sliding can be observed inside the alumina grains (Fig. 11). The forming mechanism for these kinds of dislocation patterns is complicated. However, the elastic strain energy can be deposited in the dislocation, which puts the dislocation in a substable state [25]. When the crack reaches the dislocation, some of the fracture energy can absorbed through the crack deformation. The propagating crack will have pinned and the fracture toughness of the material will increase. Also, it is clear that tantala doped samples show higher fracture toughness results than niobia ones. This could be attributed to the higher densification of tantala-doped samples.

CONCLUSIONS

1. Doping with Ta_2O_5 has much better effect on densifying α- Al_2O_3 than Nb_2O_5.The difference in the relative density is clear at lower weight percentages (0.25% and 0.5%) of dopant oxides while it is small at the high percentage of doping (0.75%), (ρ_d = 98.75 % and 98.66 % for Ta_2O_5 and Nb_2O_5 respectively).

2. Nb_2O_5 was observed at the triple junctions and the intergranular regions of the Al_2O_3 grains. Increasing the Nb_2O_5 content led to the formation of a rare-earth-containing liquid phase in the samples.

3. Even with small contents of Nb_2O_5 and Ta_2O_5, the bending strength, hardness and fracture toughness of alumina matrix ceramic bodies were all notably

improved. Ta_2O_5 has much better effect in improving the mechanical properties rather than Nb_2O_5.

REFERENCES

[1] K.L. Gavrilov, S.J. Bennison, K.R. Mikeska, J.M. Chabala and R. Levi-Setti, "Silica and magnesia dopant distributions in alumina by high-resolution scanning secondary ion mass spectrometry", J. Am. Ceram. Soc., Vol. 82, No. 4, pp. 1001-1008 (1999).

[2] C.W. Park and D.Y. Yoon, "Effect of SiO_2, CaO and MgO additions on the grain growth of alumina", J. Am. Ceram. Soc., Vol. 83, No. 10, pp. 2605-2608 (2000).

[3] J. Cho, H.M. Chen, M.P Harmer and J.M. Rickman, "Influence of yttrium doping on grain misorientation in alumina oxide", J. Am. Cerm. Soc., Vol. 81, No. 11, pp. 3001-3004 (1998).

[4] A.M. Thompson, K.K. Soni, H.M. Chen, M.P. Harmer, D.B. Williams, J.M. Chabala and R. Levi-Setti, "Dopants distributions in rare –earth-doped alumina", J. Am. Ceram. Soc., Vol. 80, No. 2, pp. 373-376 (1997).

[5] J. Cho, M.P. Harmer, H.M. Chen, J.M. Rickman and A.M. Thompson, "Effect of yttrium and lanthanum on the tensile creep behavior of aluminum oxide", J. Am. Ceram. Soc., Vol. 80, No. 4, pp. 1013-1017 (1997).

[6] D.A. Rani, Y. Yoshizawa, K. Hirao and Y. Yamauchi, "Effect of rare-earth dopants on mechanechal properties of alumina", J. Am. Ceram. Soc., Vol. 87, No. 2, pp. 289-292 (2004).

[7] Z. Xihua, L. Changxia, L. Musen and Z. Jianhua, "Research on toughening mechanisms of alumina matrix ceramic composite materials improved by rare earth additives", J. Rare earth., Vol. 26, No. 2, pp. 367-370 (2008).

[8] C-M. Wang, H.M. Chan and M.P. Harmer, "Effect of Nd_2O_3 doping on the densification and abnormal grain growth behavior of high-purity alumina", J. Am. Ceram. Soc., Vol. 87, No. 3, pp. 378-383 (2004).

[9] A. Odaka, T. Yamaguchi, T. Fujita, S. Taruta and K. Kitajima, "Densification of rare earth (Lu, Gd, Nd) – doped alumina nanopowders obtained by a sol-gel route under seeding", Powder Technol., Vol. 193, No. 1, pp. 26-31 (2009).

[10] J. Fang, A.M. Thompson, M.P. Harmer and H.M. Chan, "Effect of yttrium and lanthanum on the final-stage sintering behavior of ultrahigh-purity alumina", J. Am.Ceram. Soc., Vol. 80, No. 8, pp. 2005-2012 (1997).

[11] G.D. West, J.M. Perkins and M.H. Lewis, "The effect of rare earth dopants on grain boundary cohesion in alumina",. J. Eur. Ceram. Soc., Vol. 27, No. 4, pp. 1913-1918 (2007).

[12] C. Xu, C. Huang and X. Ai, "Toughening and strengthening of advanced ceramics with rare earth additives", Ceram. Int., Vol. 32, No. 4, pp. 423-429 (2006).

[13] G.R. Anstis, P. Chantikul, B.R. Lawn and D.B. Marshall, "A critical evaluation of indentation techniques for measuring fracture toughness: I, Direct crack measurement", J. Am. Ceram. Soc., Vol. 64, No. 9, pp. 533-538 (1981).

[14] D. Tang, H. Lim, K. Lee, C. Lee and W. Cho, "Evaluation of mechanical reliability of zirconia-toughened alumina composites for dental implants", Ceram. Int., Vol. 38, No. 3, pp. 2429-2436 (2012).

[15] D. Munz and T. Fett, "Ceramics: mechanical properties, failure behaviour, materials selection", Berlin, Springer-Verlag; 1999.

[16] T.P. Hoepfner and E.D. Case, "The influence of the microstructure on the hardness of sintered hydroxyapatite", Ceram. Int., Vol. 29, No. 6, pp. 699-707 (2003).

[17] N. Louet, H. Reveron and G. Fantozzi, "Sintering behaviour and microstructural evolution of ultrapure α-alumina containing low amounts of SiO_2", J. Eur. Ceram. Soc., Vol. 28, No. 1, pp. 205-215 (2008).

[18] L. Gremillard, T. Epicier, J. Chevalier and G. Fantozzi, "Effect of cooling rate on the location and chemistry of glassy phases in silica-doped 3Y-TZP ceramics", J. Eur. Ceram. Soc., Vol. 25, No. 6, pp. 875-882 (2005).

[19] O. Yamagguchi, D. Tomihisa and K. Shimizu, "Formation and transformation of δ- Nb_2O_5 solid solutions in the system Nb_2O_5 - Al_2O_3", Z. Anorg. Allg. Chem., Vol. 569, No. 1, pp 177-182 (1989).

[20] B.F. Pedersen, "The crystal structure of aluminum niobium oxide ($AlNbO_4$) ", Acta. Chem. Scand., Vol. 16, pp. 421-430 (1962).

[21] Y. Yang, Y. Wang, W. Tian, Z. Wang, Y. Zhao and J. Wang, "Reinforcing and toughening alumina/titania ceramic composites with nano-dopants from nanostructured composite powders", Mater. Sci. Eng. A., Vol. 508, No. 1-2, pp. 161-166 (2009).

[22] K. Niihara, "New design concept of structural ceramics — ceramic nanocomposites", J. Ceram. Soc. Jpn. Int. Ed., Vol. 99, pp. 945-952 (1991).

[23] N.A. Rejab, A.Z.A. Azhar, M.M. Ratnam and Z.A. Ahmad, "The effects of CeO_2 addition on the physical, microstructural and mechanical properties of yttria stabilized zirconia toughened alumina (ZTA) ", Int. J. Refract. Met. Hard Mater., Vol. 36, pp. 162-166 (2013).

[24] T. Oungkulsolmongkol, P. Salee-art and W. Buggakupta, "Hardness and Fracture Toughness of Alumina-Based Particulate Composites with Zirconia and Strontia Additives", J. Mater. Sci. Min., Vol. 20, No. 2, pp 71-78 (2010).

[25] X. Chonghai, "Study on microstructure of alumina based rare earth ceramic composite", J. Rare. Earth, Vol. 24, No. 1, pp. 217-222 (2006).

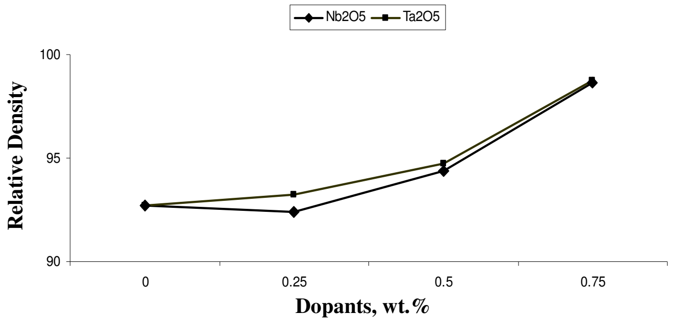

Fig. 1. Relative density of the studied bodies fired at 1650 ºC.

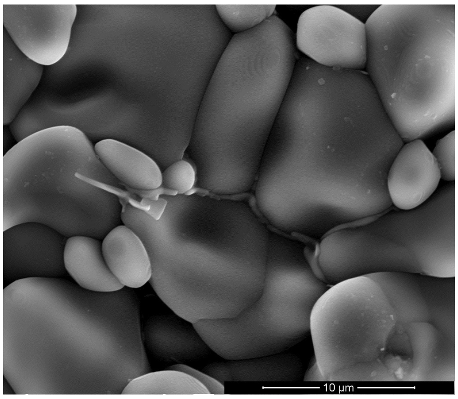

Fig. 2. Solid solution formed at the grain-boundary triple junctions of Nb_2O_5 doped alumina.

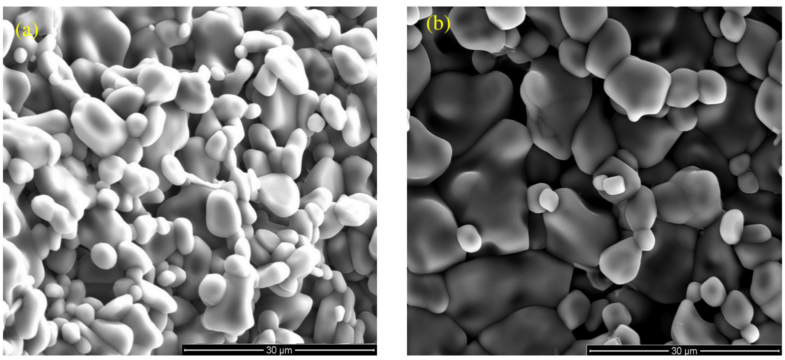

Fig. 3. Average grain size of Al_2O_3 (a)Ta^{5+} doped (b) Nb^{5+} doped samples.

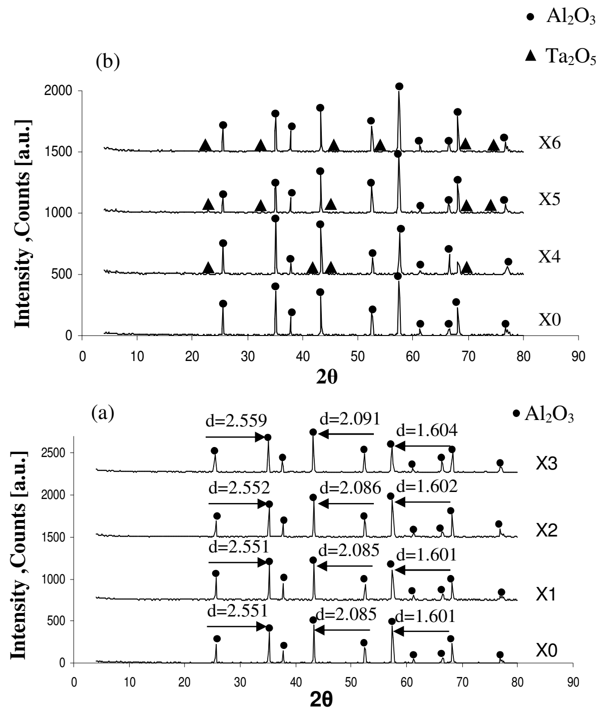

Fig. 4. XRD pattern of (a) Al_2O_3/ Nb_2O_5 bodies, (b) Al_2O_3/ Ta_2O_5 bodies fired at 1650º C.

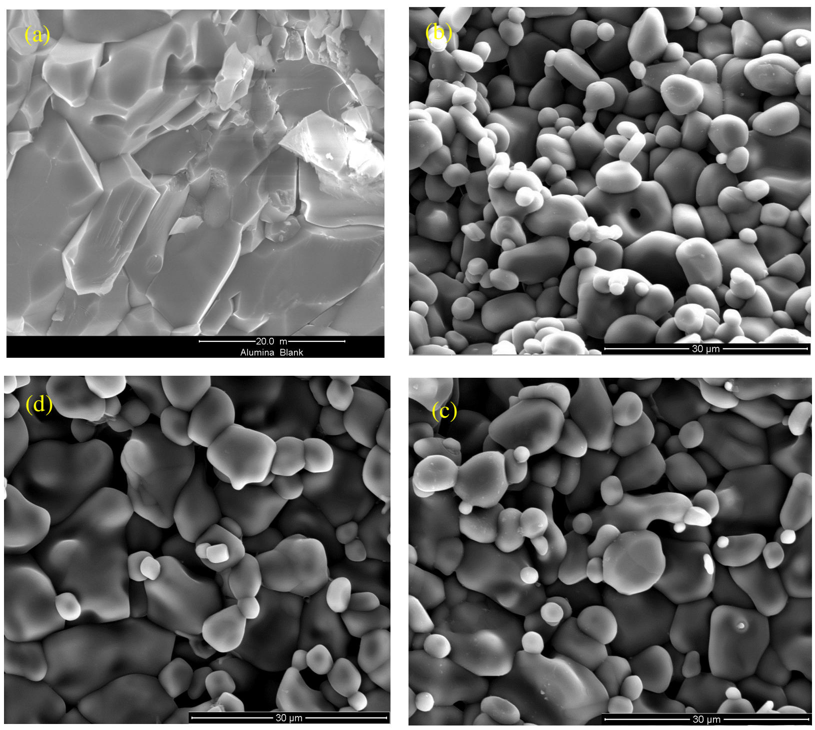

Fig. 5. SEM micrograph of X0 (a), X1(b), X2 (c) and X3 (d) samples fired at 1650ºC.

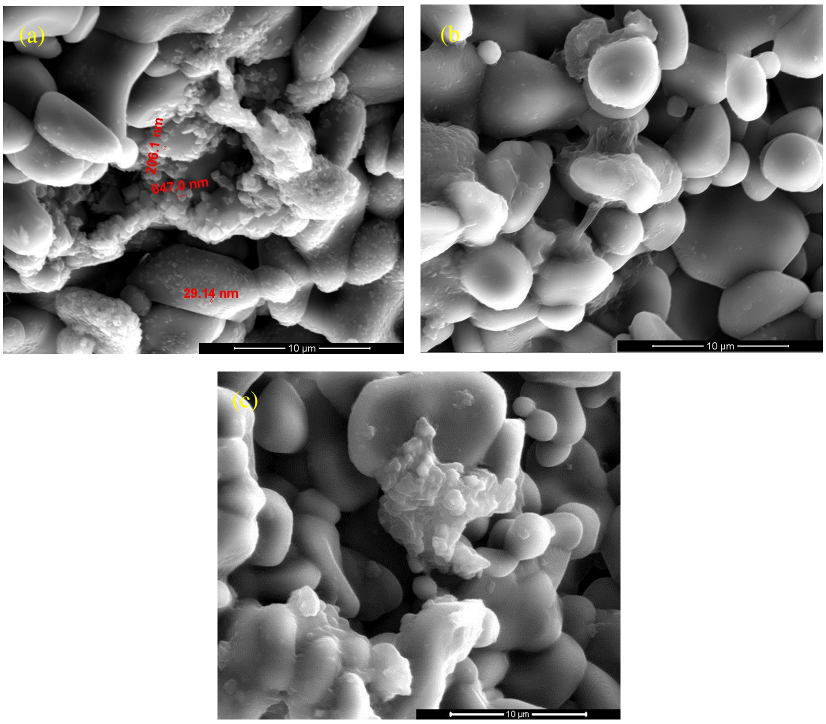

Fig. 6. SEM micrograph of X4 (a), X5(b) and X6 (c) samples fired at 1650ºC.

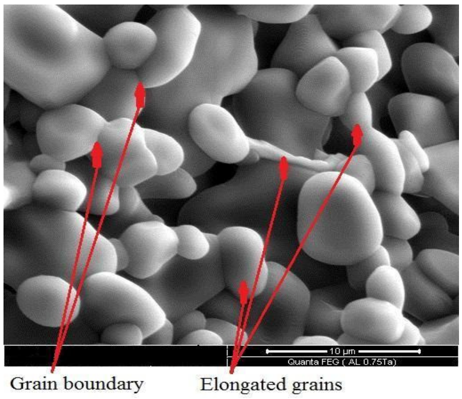

Fig. 7. SEM micrograph of X3 sample fracture surface indicating the presence of the elongated grains and the free grain boundary.

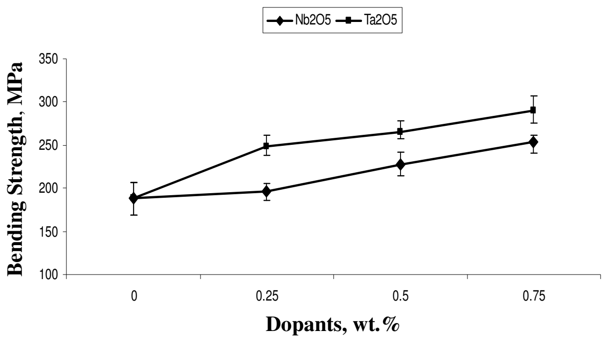

Fig. 8. Effect of dopants content on the bending strength of composites fired at 1650ºC.

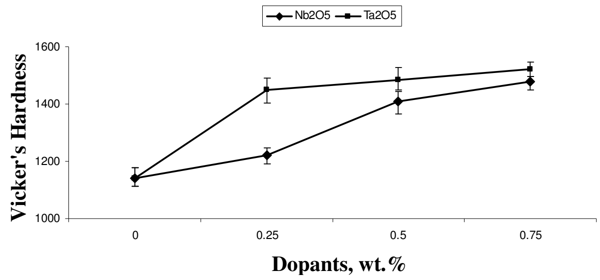

Fig. 9. Effect of dopant content on the Vickers Hardness of composites sintered at 1650 ºC.

Table 1. Compositions of Nb_2O_5 and Ta_2O_5 doped Al_2O_3 batches, wt.%.

Batch Symbol	Al_2O_3, wt.%,	Nb_2O_5, wt.%,	Ta_2O_5, wt.%,
Xo	100	____	____
X1	100	0.25	____
X2	100	0.5	____
X3	100	0.75	____
X4	100	____	0.25
X5	100	____	0.5
X6	100	____	0.75